JACS
JOURNAL OF THE AMERICAN CHEMICAL SOCIETY
Article
pubs.acs.org/JACS

Two Tetra-Cd^{II}-Substituted Vanadogermanate Frameworks

Jian Zhou,[†,§] Jun-Wei Zhao,[†,‡] Qi Wei,[†] Jie Zhang,[†] and Guo-Yu Yang*[,†]

[†]State Key Laboratory of Structural Chemistry, Fujian Institute of Research on the Structure of Matter, Chinese Academy of Sciences, Fuzhou, Fujian 350002, China

[‡]Henan Key Laboratory of Polyoxometalate Chemistry, College of Chemistry and Chemical Engineering, Henan University, Kaifeng, Henan 475004, China

[§]Key Laboratory of Green Synthesis and Applications, College of Chemistry, Chongqing Normal University, Chongqing 401331, China

Supporting Information

ABSTRACT: Two new tetra-Cd^{II}-substituted vanadogermanate frameworks $\{(CdX)_4Ge_8V^{IV}{}_{10}O_{46}(H_2O)[V^{III}(H_2O)_2]_4(GeO_2)_4\}\cdot 8H_2O$ (X = ethylenediamine (en, **1**) and 1,2-diaminopropane (dap, **2**)) were hydrothermally prepared and characterized by IR spectra, elemental analysis, powder X-ray diffraction (PXRD), energy-dispersive X-ray spectroscopy (EDX), X-ray photoelectron spectroscopy (XPS), thermogravimetric analysis (TGA), and X-ray single-crystal diffraction. Both are isomorphic, and their 3-D frameworks are made up of tetra-Cd^{II}-substituted $\{(CdX)_4Ge_8V^{IV}{}_{10}O_{46}(H_2O)\}^{12-}$ fundamental building units interconnected through planar tetra-V^{III} $[V^{III}{}_4O_2(H_2O)_8]^{8-}$ clusters and tetrahedral GeO_4 bridges. In the unique $\{(CdX)_4Ge_8V^{IV}{}_{10}O_{46}(H_2O)\}^{12-}$ cage, four $[Ge_2O_7]$ dimers and four CdO_4N_2 trigonal prisms are alternately concatenated by μ_3-O bridges to create a round $\{Ge_8Cd_4O_{28}(X)_4\}^{16-}$ fragment, five VO_5 groups are linked by sharing edges to generate a pentanuclear $[V_5O_{17}]$ subunit, and then the $\{Ge_8Cd_4O_{28}(X)_4\}^{16-}$ fragment is sandwiched by two V_5O_{17} subunits *via* sharing O-atoms producing a D_{4h}-symmetric $\{(CdX)_4Ge_8V^{IV}{}_{10}O_{46}(H_2O)\}^{12-}$ cage with a free water molecule located at the center. As we know, both display unprecedented 3-D organic−inorganic hybrid frameworks built up from the largest number of transition-metal-substituted vanadogermanate $\{(CdX)_4Ge_8V^{IV}{}_{10}O_{46}\}^{12-}$ cluster shells linked by both GeO_4 tetrahedra and rare $[V^{III}{}_4O_2(H_2O)_8]^{8-}$ clusters. Magnetic measurements reveal the antiferromagnetic couplings within the magnetic vanadium centers.

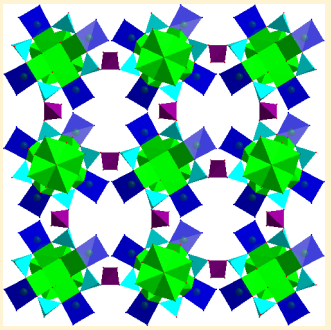

INTRODUCTION

Integration of heteroatoms into polyoxometalate (POM) backbones is a feasible and promising strategy for making a new class of heteropolyoxometalates, which is of high relevance due to their abundant structures and conceivable applications from magnetism/catalysis to medicine/electrochemistry.[1,2] Vanadium is of particular interest since it shows flexible coordination as well as a great variety of chemical valence states. During the past several years, significant progress has already been made in the syntheses of vanadoarsenates (VAOs)[3] and vanadoantimonates[4] by incorporating group 15 elements (As^{III}/Sb^{III}) into the well-known Keggin $[V_{18}O_{42}]$ cluster shell, where the $[As^{III}{}_2O_5]/[Sb^{III}{}_2O_5]$ dimers, formed by two vertex-sharing $[AsO_3]/[SbO_3]$ trigonal pyramids, are substituted for the VO_5 groups on the $[V_{18}O_{42}]$ shell. However, they are not effective on making high-dimensional frameworks because of the presence of the electron lone pairs on As^{III}/Sb^{III} atoms. The $[Si_2O_7]/[Ge_2O_7]$ dimers made up of two SiO_4/GeO_4 tetrahedra, obviously superior to the $[As_2O_5]/[Sb_2O_5]$ units, can increase the likelihood of producing extended structures *via* self-condensation of $[Si_2O_7]/[Ge_2O_7]$ units or offering good donors for electrophilic metal ions. Despite the fact that some vanadosilicates (VSOs) and vanadogermanates (VGOs) have been reported,[5] little progress has been made in making 3-D VSOs/VGOs.[6] More importantly, the construction of 3-D frameworks based on the self-condensation of $[Si_2O_7]/[Ge_2O_7]$ units or the connection of other cluster linkers has not been documented to date.

Moreover, it is expected that the second transition-metal (TM) ions are further incorporated into heteropolyoxovanadate (HPOV) skeletons, which may produce fascinating hybrids with novel frameworks and performances. Nevertheless, almost no progress has been made in investigating TM-substituted HPOVs because it is quite difficult to isolate the stable vacant HPOV precursors in contrast to a large number of reported TM-substituted polyoxotungstates.[2] With the aim of making TM-substituted HPOVs, we began to exploit the VAO system in the presence of the second TM cations by using a hydrothermal technique and successfully obtained a class of mono- and di-TM-substituted VAOs (TM = Zn^{II}, Cd^{II}, Ni^{II}).[7] Subsequently, similar conditions were employed to make Zn-/Cd-substituted VAOs with mixed organic amines.[8] Compared to TM-substituted VAOs, TM-substituted VGOs are scarce and only a di-Cd^{II}-substituted VGO $\{[(en)_2H_8Cd_2Ge_8V_{12}O_{48}][Cd(en)_2]_2\}\cdot 7H_2O$ has been made.[6c] Notably, the largest number

Received: December 30, 2013
Published: March 18, 2014

   dx.doi.org/10.1021/ja413218w | J. Am. Chem. Soc. 2014, 136, 5065−5071

Table 1. Summary of Crystal Data of Compounds 1 and 2

	1	2
formula	$C_8H_{66}Cd_4Ge_{12}N_8O_{71}V_{14}$	$C_{12}H_{74}Cd_4Ge_{12}N_8O_{71}V_{14}$
fw	3444.81	3500.63
crystal system	tetragonal	tetragonal
space group	*P*4/*mnc*	*P*4/*mnc*
a, Å	17.682(4)	17.985(3)
b, Å	17.682(4)	17.985(3)
c, Å	14.556(3)	14.597(3)
V, Å^3	4551.0(17)	4721.6(13)
Z	2	2
T, K	293(2)	293(2)
calcd density, g·cm^{-3}	2.489	2.462
abs coeff, mm^{-1}	6.269	6.044
F(000)	3204	3188
2θ(max), deg	49.99	49.99
total reflns colected	28 691	27 951
unique reflns	2037	2123
no. of param	151	151
$R_1[I > 2\sigma(I)]$	0.0523	0.0487
wR_2	0.1342	0.1415

of TM ions in a single VGO cluster is only 2 to date. Therefore, the syntheses of novel VGOs with a larger number of TM atoms have become an attractive and challenging goal.

With regard to all aspects stated above, we began to explore and make high-dimensional TM-substituted VGOs based on the following considerations: (a) Incorporation of TM ions into VGO cages may previously create unseen TM-substituted HPOVs coupled with unexpected properties; (b) the $[Ge_2O_7]$ units can be further condensed or offer specific coordination sites for TM connectors into extended frameworks. Herein, the syntheses, crystal structures, and magnetic properties of two novel 3-D tetra-Cd^{II}-substituted VGOs $\{(CdX)_4Ge_8V^{IV}{}_{10}O_{46}(H_2O)[V^{III}(H_2O)_2]_4(GeO_2)_4\}\cdot 8H_2O$ [X = ethylenediamine (en, **1**) and 1,2-diaminopropane (dap, **2**)] are reported, which are the first examples of 3-D frameworks based on the largest number of TM-substituted VGO $\{(CdX)_4Ge_8V^{IV}{}_{10}O_{46}\}^{12-}$ cluster shells linked by two kinds of the linkers, GeO_4 tetrahedra and $[V^{III}{}_4O_2(H_2O)_8]^{8-}$ clusters.

EXPERIMENTAL SECTION

Materials and Methods. The chemicals are of analytical grade and were commercially purchased, without further purification. Elemental analyses were performed by a Vario EL III elemental analyzer for C/H/N and a Jobin Yvon ultima 2 inductively coupled plasma optical emission spectrometry spectrometer for Cd/Ge/V, respectively. IR spectra were recorded on an ABB Bomen MB 102 series IR spectrophotometer (KBr pellets) over the region 400−4000 cm^{-1}. XPS data were obtained from an Axis Ultra X-ray photoelectron spectrometer. TGA measurements were carried out by a Mettler Toledo TGA/SDTA 851^e analyzer under a flowing air atmosphere between 25 and 1000 °C at a heating speed of 10 °C·min^{-1}. Magnetic susceptibility data were measured with a Quantum Design MPMS XL-5 SQUID magnetometer on polycrystalline samples in an external magnetic field of 1 kOe at 2−300 K. All the magnetic susceptibility data were corrected from diamagnetic contributions estimated from Pascal's constants. PXRD data were obtained by a Bruker D8 Advance XRD diffractometer with Cu Kα radiation (λ = 1.54056 Å). EDX spectroscopy was recorded on a JEOL JSM-6700F field-emission scanning electron microscope.

Synthesis of 1. NH_4VO_3 (0.0216 g, 0.18 mmol), GeO_2 (0.0380 g, 0.37 mmol), $CdCl_2\cdot 2.5H_2O$ (0.0507 g, 0.18 mmol), H_3BO_3 (0.0158 g, 0.26 mmol), and en (0.10 mL) were added to H_2O (5 mL) solution with stirring. The final mixture (pH 9.7−10) was moved to a 35 mL Teflon-lined autoclave, sealed, and kept at 170 °C for 96 h, and then it was cooled to ambient temperature. Red block-shaped crystals were harvested (Yield: 36.2% on the base of GeO_2). Similarly, **1** can also be made by using H_2CO_4 in place of H_3BO_3, but the yield and crystallinity of **1** are lowered. Notably, the crystallinity of **1** was highly sensitive to the pH of the reaction system, and only varied from 9.7 to 10. When the pH was beyond this range, **1** could not be afforded. Anal. Calcd (%) for $C_8H_{66}Cd_4Ge_{12}N_8O_{71}V_{14}$: C, 2.79; H, 1.93; N, 3.25; Cd, 13.05; Ge, 25.29; V, 20.70. Found: C, 2.84; H, 2.15; N, 3.31; Cd, 12.63; Ge, 24.88; V, 20.41. IR (KBr): ν = 3341(m), 3275(m), 3159(m), 2926(w), 2876(w), 1634(m), 1590(m), 1459(w), 1394(m), 1329(w), 1256(w), 1002(m), 944(m), 777(s), 668(w), 551(s), 472(m) cm^{-1}.

Synthesis of 2. NH_4VO_3 (0.0406 g, 0.35 mmol), GeO_2 (0.0714 g, 0.68 mmol), $CdCl_2\cdot 2.5H_2O$ (0.1432 g, 0.49 mmol), $H_2C_2O_4\cdot 2H_2O$ (0.0608 g, 0.48 mmol), and dap (0.40 mL) were added in H_2O (5 mL) solution with stirring. The final mixture (pH 9.7−10) was sealed in a 35 mL Teflon-lined autoclave, kept at 170 °C for 96 h, and then cooled to ambient temperature. Red block-shaped crystals were afforded (Yield: 51.6% on the base of GeO_2). Anal. Calcd (%) for $C_{12}H_{74}Cd_4Ge_{12}N_8O_{71}V_{14}$: C, 4.12; H, 2.13; N, 3.20; Cd, 12.84; Ge, 24.90; V, 20.37. Found: C, 4.18; H, 2.31; N, 3.31; Cd, 12.03; Ge, 24.36; V, 20.22. IR (KBr): ν = 3321(m), 3265(m), 3196(m), 2963(w), 2928(w), 1635(m), 1585(m), 1456(w), 1386(m), 1346(w), 1304(w), 1201(w), 974(m), 939(m), 774(s), 678(w), 547(s), 479(m) cm^{-1}.

X-ray Crystallographic Determination. Intensity data of **1** and **2** were collected on a Rigaku Mercury CCD diffractometer equipped with graphite monochromated Mo Kα radiation (λ = 0.71073 Å) at 293(2) K. Routine Lorentz polarization and absorption corrections were applied. Both structures were solved by direct methods and refined by the full-matrix least-squares technique with SHELXL-97. The H-atoms of the water molecules were not located. H-atoms of the C/N atoms in **1** were geometrically placed and isotropically refined as riding atoms. For **2**, H-atoms on C/N atoms of the disordered dap ligands were not added. Crystallographic data for **1** and **2** are illustrated in Table 1. The CCDC numbers are 725351 and 948521 for **1** and **2**, respectively.

RESULTS AND DISCUSSION

Structural Description. **1** and **2** were made via hydrothermal reactions of GeO_2, NH_4VO_3, and $H_3BO_3/H_2C_2O_4\cdot 2H_2O$ in an amine−H_2O mixed solvent. Although H_3BO_3 is not incorporated into the final structures, attempts to obtain both **1**

dx.doi.org/10.1021/ja413218w | J. Am. Chem. Soc. 2014, 136, 5065−5071

and **2** proved fruitless in the absence of H_3BO_3 or by the addition of other strong acids (such as HCl, HNO_3, and H_2SO_4) instead of H_3BO_3 under hydrothermal conditions, showing that the weak acid H_3BO_3 or $H_2C_2O_4{\cdot}2H_2O$ may act as structure directing agents in the reaction process. In addition, our many paralleling experiments verified that the incorporated Cd^{2+} ions cannot be replaced by other TM ions such as Mn^{2+}, Co^{2+}, Ni^{2+}, Zn^{2+}, and Fe^{2+} under similar reaction conditions, the primary possible reason of which being that the Cd^{2+} ions in **1** and **2** adopt the trigonal prismatic geometry coordinating to the backbone of vanadogermanates. However, it is difficult for other TM cations to utilize the trigonal prism configurations, thus leading to the irreplaceability of Cd^{2+} ions with other TM ions. Moreover, in the reported di-Cd^{II}-substituted VGO $\{[(en)_2H_8Cd_2Ge_8V_{12}O_{48}][Cd(en)_2]_2\}\cdot 7H_2O$,[6c] the substituted Cd^{2+} ions also display the trigonal prisms, which further supports our above speculation. Actually, unsaturated complex $[TM(amine)_x]^{2+}$ (TM = Mn^{2+}, Co^{2+}, Ni^{2+}, Zn^{2+}, Fe^{2+} ; amine = chelating amines) cations usually act as bridges or pendants,[3,4,6b] but it is very difficult for them to substitute the VO_5 groups on the skeleton of the $[V_{18}O_{42}]$ cage. The experimental and simulated PXRD patterns match well, suggesting that the samples are pure (Figure S1, Supporting Information).

Since **1** and **2** are isomorphic, herein, we only discussed the structure of **1**. **1** crystallizes in the high-symmetric tetragonal space group *P*4/*mnc*. The structure of **1** is built by tetra-Cd^{II}-substituted $\{[Cd(en)]_4Ge_8V^{IV}{}_{10}O_{46}(H_2O)\}^{12-}$ ($\{\mathbf{Cd_4Ge_8V_{10}}\}$) basic building units, which are interconnected *via* planar tetra-V^{III} $[V^{III}{}_4O_2(H_2O)_8]^{8-}$ ($\{\mathbf{V_4}\}$) clusters and tetrahedral GeO_4 bridges giving rise to an interesting 3-D organic−inorganic hybrid framework. The unique $\{\mathbf{Cd_4Ge_8V_{10}}\}$ cage contains ten condensed VO_5 square pyramids, four CdO_4N_2 trigonal prisms, and eight GeO_4 tetrahedra (Figures 1a−c): the CdO_4N_2 trigonal prism contains two nitrogen and four bridging oxygen atoms from one en ligand and four adjacent VO_5 groups, respectively; two GeO_4 groups are condensed by corner-sharing to afford the $[Ge_2O_7]$ dimer; four $[Ge_2O_7]$ dimers and four CdO_4N_2 trigonal prisms are alternately joined by the μ_3-O bridges to create a circular $\{Ge_8Cd_4O_{28}(en)_4\}^{16-}$ ($\{\mathbf{Cd_4Ge_8}\}$) fragment (Figure 1a); five VO_5 groups are linked by sharing edges to form a pentanuclear $[V_5O_{17}]$ fragment (Figures 1b, S2a, Supporting Information); and then the $\{\mathbf{Cd_4Ge_8}\}$ fragment is sandwiched by two $\{V_5O_{17}\}$ fragments *via* sharing O-atoms producing a D_{4h}-symmetric $\{\mathbf{Cd_4Ge_8V_{10}}\}$ cage with a free water molecule at the center (Figures 1c, S2b, Supporting Information). This cage is closely related to the $[V_{12}Ge_8O_{48}]$ shell in $K_5H_8Ge_8V_{12}SO_{52}{\cdot}10H_2O$ (Figure 2d),[5a] so it can also be considered that four $[Cd(en)]^{2+}$ ions replace four V=O caps located between adjacent $[Ge_2O_7]$ units on the $[V_{12}Ge_8O_{48}]$ shell to form the hybrid $\{\mathbf{Cd_4Ge_8V_{10}}\}$ shell, in which the two quadrate windows are further covered by two VO_5 polyhedra forming a hybrid tetra-Cd^{II}-substituted $\{\mathbf{Cd_4Ge_8V_{10}}\}$ cluster (Figure 2g). So far, though a few spherical TM-substituted VAOs and VGOs (Figure 2f) have been reported,[7,6c] the number of TM ions is no more than two; however, the number of Cd^{II} ions in **1** is up to four. Therefore, **1** is the first example of the highest number of TMs in $[V_{18}O_{42}]$ (Figure 2a) derivatives. The configuration of such a cage in **1** significantly differs from those reported for VGO cages $[V_{16}Ge_4O_{46}]$ (Figure 2b),[5a] $[Ge_6V_{15}O_{48}]$ (Figure 2c),[6c] $[Ge_8V_{14}O_{50}]$ (Figure 2d),[5a,b] and $[V_{12}Ge_8O_{48}]$ (Figure 2e),[5a] which are typical derivatives of the $[V_{18}O_{42}]$ clusters by replacing V=O groups with $\{Ge_2O(OH)_2\}/\{Ge_2O_3\}$ groups.[5] As a result, the $\{\mathbf{Cd_4Ge_8V_{10}}\}$ (Figures 1c, 2e) cluster in **1** is an absolutely novel structural motif.

Besides the large $\{\mathbf{Cd_4Ge_8V_{10}}\}$ cluster, another interesting $\{\mathbf{V_4}\}$ cluster is observed and formed by four $\{V^{III}O_6\}$ octahedra by sharing edges and corners (Figure 1d). Four V^{III} atoms are aligned in a planar quadrangular motif with V···V distances of 2.467(3) Å. Two terminal oxygen atoms of two $V^{IV}O_5$ square pyramids cap the quadrangle at the top and bottom, showing an uncommon μ_5-O atom coordination mode. Four H_2O molecules bridge four V···V edges, respectively, and two H_2O molecules locate at two terminal positions of each V^{III} atom. The V(3)−O(9/10) distances are in the range 1.939(17)−

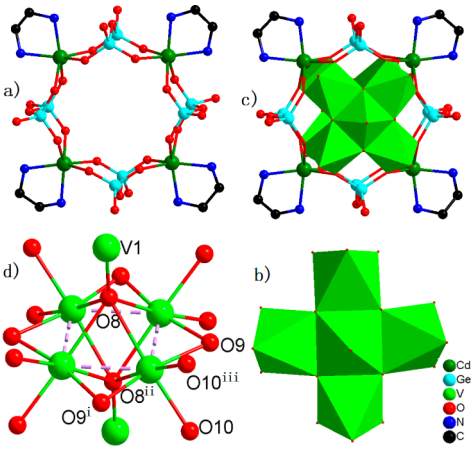

Figure 1. Structural views of **1**. (a) The circular $\{Ge_8Cd_4O_{28}(en)_4\}^{16-}$ fragment. (b) The pentanuclear V_5O_{17} fragment. (c) The $\{[Cd(en)]_4Ge_8V^{IV}{}_{10}O_{46}(H_2O)\}^{12-}$ cluster. (d) The $[V^{III}{}_4O_2(H_2O)_8]^{8-}$ cluster in **1** showing the μ_5-O coordination mode (symmetric operation code: (i) $1+x, 1-y, z$; (ii) $-x, 2-y, -z$; (iii) $x, y, -z$).

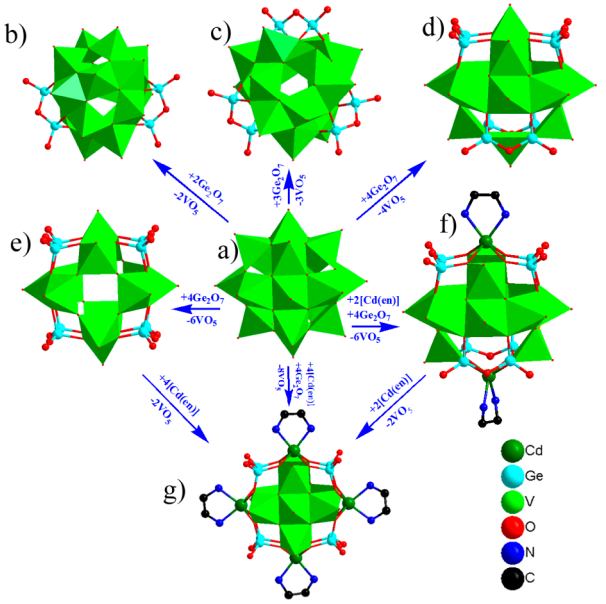

Figure 2. Combined polyhedral/ball-and-stick representations of known VGO cluster cages: (a) $[V_{18}O_{42}]$ cage, (b) $[V_{16}Ge_4O_{46}]$ cage, (c) $[Ge_6V_{15}O_{48}]$ cage, (d) $[V_{14}Ge_8O_{50}]$ cage, (e) $[V_{12}Ge_8O_{48}]$ cage, (f) $[(en)_2Cd_2Ge_8V_{12}O_{48}]$ cage, and (g) $\{Cd_4Ge_8V_{10}\}$ cage in **1**.

dx.doi.org/10.1021/ja413218w | J. Am. Chem. Soc. 2014, 136, 5065−5071

2.039(19) Å, which coincide with the corresponding bond lengths of the regular $[V^{III}O_6]$ octahedra,[9] but the slightly elongated V(3)−O(8) distance (2.278(8) Å) might be due to the influence of the O8 atom coordinating to five V-atoms. A similar phenomenon is observed in other polyoxovanadates.[10] If the $\{\mathbf{V_4}\}$ cluster is regarded as an isolated structure, it would have the point group symmetry of D_{4h}. Among reported oxo-/thio-V_4 clusters, most of them own a tetrahedral V_4 core,[11] and circle/butterfly/cuprous oxo-V_4 clusters have also been made.[12] But no planar quadrangular oxo-V_4 cluster has been observed to date. Therefore, the $\{\mathbf{V_4}\}$ cluster in **1** shows another innovative structural motif. In addition, bond valence sum ($\sum_s$) calculations[13] indicate that the chemical valences of V1, V2, and V3 centers are +4, +4, and +3 in **1** and **2** (Table S1, Supporting Information). This assignment was also confirmed by XPS spectra (Figure S3, Supporting Information). The peaks of $V2p_{3/2}$ and $V2p_{1/2}$ appearing at 514.5 and 522.0 eV for **1** and 514.6 and 522.1 eV for **2** illuminate the existence of the V^{III} ions, whereas the signals of $V2p_{3/2}$ and $V2p_{1/2}$ centered on 515.4 and 523.1 eV for **1** and 515.5 and 523.1 eV for **2** expound the existence of the V^{IV} ions. These binding energies are consistence with those reported values.[14] Furthermore, in XPS spectra, the binding-energy discrepancy (Δ) between O1s and $V2p_{3/2}$ levels has often served in identifying the chemical valences of vanadium ions within oxo-vanadium clusters. The Δ values of V^{3+} and V^{4+} are 14.9 and 14.0 eV for **1** and 14.8 and 13.9 eV for **2**, respectively, and are very close to the reported Δ values of V^{3+} (14.84 eV) and V^{4+} (14.16 eV), which further indicate the coexistence of V^{3+} and V^{4+}.[14,15]

Each $\{\mathbf{Cd_4Ge_8V_{10}}\}$ cluster in **1** links adjacent ones by eight tetrahedral GeO_4 and two square $\{\mathbf{V_4}\}$ bridges (Figures 3a,b),

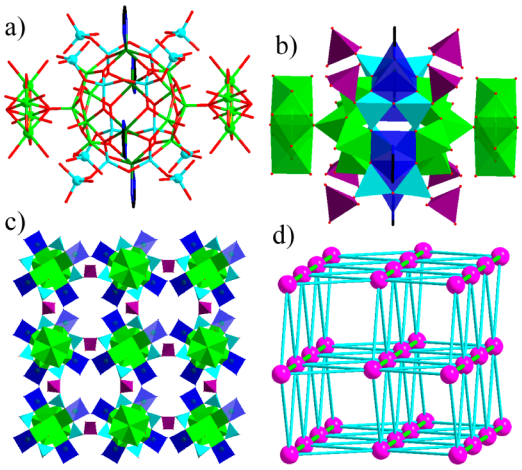

Figure 3. (a) Ball-and-stick view of the $\{Cd_4Ge_8V_{10}\}$ cluster linked by $\{V_4\}$ clusters and the bridging GeO_4 tetrahedra. (b) Polyhedral representation of the $\{Cd_4Ge_8V_{10}\}$ cluster. Dark purple/blue, $[GeO_4]$ tetrahedra; green, $[VO_x]$ polyhedra; deep blue, $[CdO_4N_2]$ polyhedra. (c) The 3-D framework constructed by bridging GeO_4 tetrahedra, $\{Cd_4Ge_8V_{10}\}$ and $\{V_4\}$ clusters. The en ligands and free water molecules are deleted for clarity. (d) The 3-D topology of **1**.

leading to a 3-D 10-connected framework accompanied by 1-D 10-membered ring (MR) dumbbell channels viewed along the [001] direction (Figure 3c). These channels are delimited by six GeO_4 tetrahedra and four CdO_4N_2 trigonal prisms with an effective cross-section size of about 4.9 × 10.5 $Å^2$, which are occupied by lattice water guests. The N-atoms of CdO_4N_2 trigonal prisms protrude into the 10-MR channels. The orientations of these dumbbell-shaped channels are perpendicular with each other. The 3-D topology of **1** can be simplified by thinking of $\{\mathbf{Cd_4Ge_8V_{10}}\}$ units as nodes and GeO_4 tetrahedra and $\{\mathbf{V_4}\}$ clusters as linkers (Figure 3d). Thus, its 3-D structure belongs to the *bct* topology with a point-symbol of $3^{12}\cdot4^{28}\cdot5^5$. If there is no bridging $\{\mathbf{V_4}\}$ cluster, a similar 3-D framework can also exist in **1** (Figure S4, Supporting Information), because each $\{\mathbf{Cd_4Ge_8V_{10}}\}$ unit has four pairs of GeO_4 tetrahedral corners available for further covalent bonding to eight GeO_4 tetrahedra to form the 3-D framework. However, the related VAOs, originating from the $[V_{18}O_{42}]$ shell through substituting two diagonal VO_5 square pyramids using $[As_2O_5]$ groups, cannot link to each other, mainly due to the fact that the unshared electron lone pair on As(III) atoms effectively terminate the expansion of the structure. The results enable us to speculate that the $[Ge_{2m}V_{16-m}O_{42+2m}]$ (m = 2, 3, 4) segments based on the $[V_{18}O_{42}]$ shell can act as specific connectors to build various 1-, 2-, and even 3-D VGOs.

The third appealing characteristic in **1** is that the bridging role of the GeO_4 tetrahedra is unfamiliar in POM chemistry while the reported 1-, 2-, and 3-D POMs are usually formed by a combination of POM units and linkers such as organic bridging ligands,[2b,16] simple metal cations,[2d,17] or complex cations.[18] Some extended lattices are built by the clusters via the oxygen atom linkers.[1b,19] A few extended frameworks are based on POM cores linked by single nonmetal tetrahedra such as PO_4^{3-} and SiO_4^{4-} anions.[20] Only one observed exception is $Cs_{10.5}[(V_{16}O_{40})(Si_{4.5}V_{1.5}O_{10})]\cdot3.5H_2O$,[5f] in which the $[V_{16}Si_4O_{46}]$ unit has four disordered $[(V_{1.5}Si_{0.5})O_4]$ nonmetal/TM tetrahedra corner-sharing with two pairs of SiO_4 tetrahedra of the shells to form the infinite chain. However, the 3-D framework of **1** is the first POM cluster unit linked by main-group metal tetrahedral GeO_4 bridges until now.

More interestingly, there are two types of the chains in **1**. One is the straight chain built by two kinds of clusters, $\{\mathbf{Cd_4Ge_8V_{10}}\}$ and $\{\mathbf{V_4}\}$, along the *c*-axis (Figure 4a). The fact that two such different cluster units are observed in an organic−inorganic hybrid HPOV **1** is rare because the most extended POM frameworks are usually based on the same cluster units.[16−20] The other is the sinusoid-like $[GeO_3]_n^{2n-}$ chain constructed by repeated corner bridging of tetrahedral GeO_4^{4-} anions. The individual chains are shifted by *c*/2 against each other and connected *via* CdO_4N_2 trigonal prisms, forming the layers with 14-MR windows in the (100) or (010) plane (Figure 4b,c). Then, such layers are linked in an antiparallel fashion via CdO_4N_2 trigonal prisms along the [100] or [010] direction to construct a 3-D framework (Figure 4d), in which there are three types of channels delimited by CdO_4N_2 trigonal prisms and GeO_4 tetrahedra. The first is the 14-MR elliptical channels along the [100] or [010] direction (Figure 4d), and the remaining two types are the 8-MR circular channels and 10-MR dumbbell channels along the *c*-axis (Figures S5a−c, Supporting Information). One $\{\mathbf{V_4}\}$ cluster links two $[V_5O_{17}]$ units to form a linear V_5O_{17}−$\{\mathbf{V_4}\}$−V_5O_{17} segment that are filled in the 14-MR channels (Figure S5e,f, Supporting Information), in which the $[V_5O_{17}]$ units interact with the pore wall *via* the covalent bonds and play a dual role in stabilizing the framework and structurally modified aspect (Figure 4e). The 10-MR dumbbell channel is built up from four $[GeO_3]_n^{2n-}$ chains linked by CdO_4N_2 trigonal prisms along the 4_1 screw axis (Figure 4f). Such a 3-D framework is closely related to those of ASU-24−26,[21] FDZG-3,[22] and NGH-5,[23] which all contain the sinusoid-like $[GeO_3]_n^{2n-}$ chains. A

dx.doi.org/10.1021/ja413218w | J. Am. Chem. Soc. 2014, 136, 5065−5071

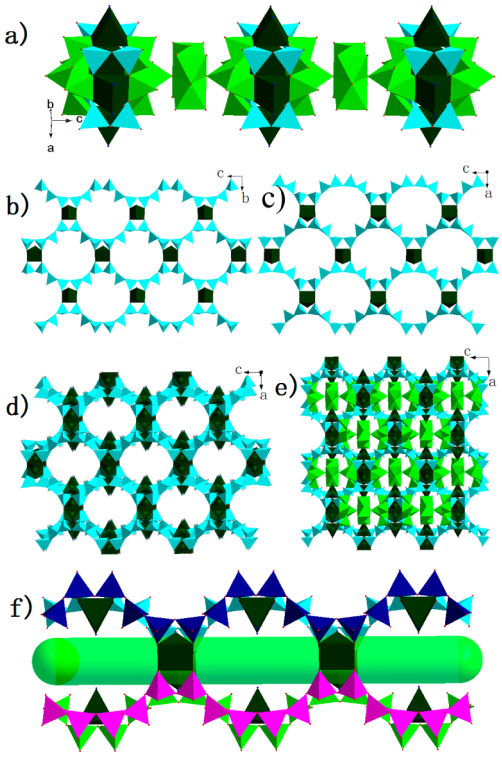

Figure 4. (a) The 1-D chain built by both $\{V_4\}$ and $\{Cd_4Ge_8V_{10}\}$ clusters. (b and c) The 2-D layers with 14-MR windows based on the combination of 1-D $[GeO_3]_n^{2n-}$ chains and $[CdO_4N_2]$ trigonal prisms. (d) The 3-D framework linked by the layers shown in Figure 4b–c, showing 14-MR channels. (e) The $\{V_4\}$ clusters and pentanuclear $[V_5O_{17}]$ units filled in 14-MR channels. (f) View of the tubular made of four $[GeO_3]_n^{2n-}$ chains marked by different colors.

common structural feature of these reported $[GeO_3]_n^{2n-}$ chains is the same periodic unit formed by three corner-sharing GeO_4 tetrahedra (Figure S6a, Supporting Information), while the $[GeO_3]_n^{2n-}$ chains in **1** exhibit a new periodic unit containing six corner-sharing tetrahedra for a complete sinusoid-like period of 11.5 Å (Figures S5d, 6b, Supporting Information). So far, only one 3-D framework cadmium-germanate was observed, in which the $[Cd_2(en)_3]^{4+}$ cations as the nonbridging groups are regularly appended to the 3-D framework,[24] while the $[Cd(en)]^{2+}$ cations in **1** as the linkers directly bond the $[GeO_3]_n^{2n-}$ chains to build the 3-D framework.

Magnetic Properties. Variable-temperature magnetic behaviors for **1** and **2** have been measured at 2–300 K in an external field of 5 kOe (Figures 5,6). At room temperature, the

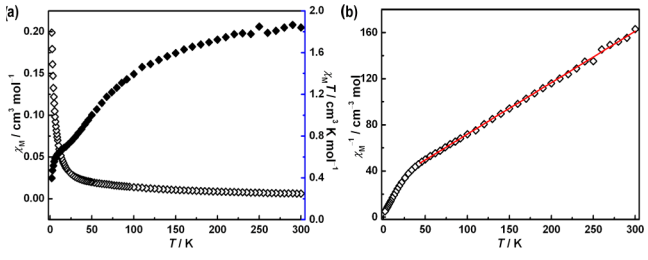

Figure 5. (a) Plot of χ_M and $\chi_M T$ versus T for **1** between 2 and 300 K. (b) Plot of χ_M^{-1} versus T for **1**. The simulation of the Curie–Weiss law to susceptibility data generates the red solid line between 38 and 300 K, giving rise to C = 2.24 $cm^3 \cdot mol^{-1} \cdot K$ and θ = −61.01 K.

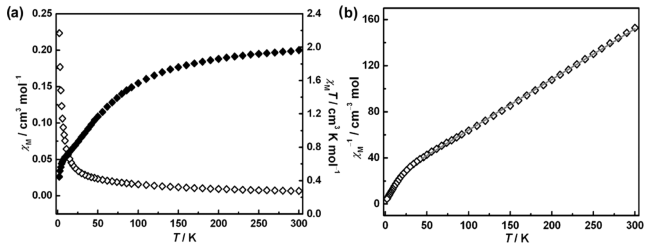

Figure 6. (a) Plot of χ_M and $\chi_M T$ versus T for **1** between 2 and 300 K. (b) Plot of χ_M^{-1} versus T for **1**. The simulation of the Curie–Weiss law to susceptibility data generates the red solid line between 34 and 300 K, giving rise to C = 2.27 $cm^3 \cdot mol^{-1} \cdot K$ and θ = −45.73 K.

$\chi_M T$ of 1.84 $cm^3 \cdot mol^{-1} \cdot K$ for **1** and 1.96 $cm^3 \cdot mol^{-1} \cdot K$ for **2** is much lower than the theoretical value of 7.45 $cm^3 \cdot mol^{-1} \cdot K$ for 10 noninteracting V^{IV} (S = 1/2) and 4 isolated V^{III} (S = 1) cations considering g = 2.00. Upon cooling, the $\chi_M T$ value declines rapidly to 0.66 $cm^3 \cdot mol^{-1} \cdot K$ for **1** and 0.72 $cm^3 \cdot mol^{-1} \cdot K$ for **2** at 12 K and then descends promptly from 12 K and reaches the minimal value of 0.39 $cm^3 \cdot mol^{-1} \cdot K$ for **1** and 0.45 $cm^3 \cdot mol^{-1} \cdot K$ for **2** at 2 K. The above profile suggests that overall antiferromagnetic couplings exist in **1** and **2**. The χ_M^{-1} versus T conforms to the Curie–Weiss law between 38 and 300 K for **1** and between 34 and 300 K for **2** with C = 2.24 $cm^3 \cdot mol^{-1} \cdot K$ and θ = −61.01 K for **1** and C = 2.27 $cm^3 \cdot mol^{-1} \cdot K$ and θ = −45.73 K for **2**, respectively, which further verify the presence of the antiferromagnetic couplings between V^{IV} and V^{III} ions in both cases.

IR Spectra and TGA. The IR spectra of **1** and **2** exhibit the characteristic vibration absorption bands of VGOs (Figure S7, Supporting Information). The strong absorption bands at 1000–944 cm^{-1} are assigned to the ν(V=O) stretching vibrations, and the absorption bands at 776–668 cm^{-1} are derived from the common contribution of the ν(Ge–O) and ν(V/Ge–O–V/Ge) stretching vibration modes.[6b,c] The resonance bands centered at 3341–3265 and 2963–2876 cm^{-1} are respectively attributable to the $\nu(NH_2)$ and $\nu(CH_2)$ stretching vibrations, which confirm the presence of organic amine groups. The broadened band centered at 3450–3433 cm^{-1} is indicative of the ν(O–H) stretching vibration in water molecules. The TGA curve of **1** (Figure S8, Supporting Information) shows a sharp weight loss of 4.94% occurring between 25 and 145 °C, corresponding to the liberation of free waters (calcd 4.71%), and then a gradual weight loss of 11.25% from 150 to 770 °C is attributed to the loss of en ligands (calcd 6.98%) and the liberation of coordinated water molecules (calcd 4.18%). For **2**, the TGA curve manifests a slow three-step weight loss process with the overall weight loss of 18.03% between 30 and 708 °C, which can be assigned to the removal of water and dap components (calcd 17.22%). The experimental values match the calculated values from their formulas.

CONCLUSIONS

We have successfully introduced the secondary TM (herein is cadmium) to a VGO cluster backbone and obtained two unprecedented 3-D tetra-Cd^{II}-substituted VGOs under hydrothermal conditions, which represent the first 3-D frameworks built by the largest number of TM-substituted VGO $\{Cd_4Ge_8V_{10}\}$ cluster shells linked by tetrahedral GeO_4 units and $\{V_4\}$ clusters. Hence, both **1** and **2** not only offer two exciting TM-substituted HPOVs but also suggest the feasibility

dx.doi.org/10.1021/ja413218w | J. Am. Chem. Soc. 2014, 136, 5065–5071

of other TM-substituted VGOs, which will broaden the frontier field of POM chemistry.

■ ASSOCIATED CONTENT

Supporting Information

One additional table and nine additional figures including XRD, IR, TG, XPS, EDX, etc. This material is available free of charge via the Internet at http://pubs.acs.org.

■ AUTHOR INFORMATION

Corresponding Author

ygy@fjirsm.ac.cn

Notes

The authors declare no competing financial interest.

■ ACKNOWLEDGMENTS

This work was supported by the NSFC (Nos. 91122028, 21221001, and 50872133), the NSFC for Distinguished Young Scholars (No. 20725101), and the 973 program (Nos. 2014CB932101 and 2011CB932504).

■ REFERENCES

(1) (a) Kikukawa, Y.; Yamaguchi, S.; Nakagawa, Y.; Uehara, K.; Uchida, S.; Yamaguchi, K.; Mizuno, N. *J. Am. Chem. Soc.* **2008**, *130*, 15872−15878. (b) Nyman, M.; Bonhomme, F.; Alam, T. M.; Rodriguez, M. A.; Cherry, B. R.; Krumhansl, J. L.; Nenoff, T. M.; Sattler, A. M. *Science* **2002**, *297*, 996−998. (c) Long, D.; Abbas, H.; Kögerler, P.; Cronin, L. *Angew. Chem., Int. Ed.* **2005**, *44*, 3415−3419. (d) Rüther, T.; Hultgren, V. M.; Timko, B. P.; Bond, A. M.; Jackson, W. R.; Wedd, A. G. *J. Am. Chem. Soc.* **2003**, *125*, 10133−10143. (e) Rhule, J. T.; Hill, C. L.; Judd, D. A. *Chem. Rev.* **1998**, *98*, 327−357. (f) Katsoulis, D. E. *Chem. Rev.* **1998**, *98*, 359−387. (f) Wang, C.-M.; Zheng, S.-T.; Yang, G.-Y. *Inorg. Chem.* **2007**, *46*, 616−618.

(2) (a) Zhao, J.-W.; Li, B.; Zheng, S.-T.; Yang, G.-Y. *Cryst. Growth Des.* **2007**, *7*, 2658−2664. (b) Zheng, S.-T.; Zhang, J.; Yang, G.-Y. *Angew. Chem., Int. Ed.* **2008**, *47*, 3909−3913. (c) Zheng, S.-T.; Yuan, D.-Q.; Jia, H.-P.; Zhang, J.; Yang, G.-Y. *Chem. Commun.* **2007**, 1858−1860. (d) Tan, H.; Li, Y.; Zhang, Z.; Qin, C.; Wang, X.; Wang, E.; Su, Z. *J. Am. Chem. Soc.* **2007**, *129*, 10066−10067. (e) Ritchie, C.; Streb, C.; Thiel, J.; Mitchell, S. G.; Miras, H. N.; Long, D.; Boyd, T.; Peacock, R. D.; McGlone, T.; Cronin, L. *Angew. Chem., Int. Ed.* **2008**, *47*, 6881−6884. (f) Streb, C.; Ritchie, C.; Long, D.; Kögerler, P.; Cronin, L. *Angew. Chem., Int. Ed.* **2007**, *46*, 7579−7582.

(3) (a) Qi, Y.; Li, Y.; Wang, E.; Jin, H.; Zhang, Z.; Wang, X.; Chang, S. *J. Solid State Chem.* **2007**, *180*, 382−389. (b) Zheng, S.-T.; Zhang, J.; Yang, G.-Y. *J. Mol. Struct.* **2004**, *705*, 127−132. (c) Cui, X.-B.; Xu, J.-Q.; Sun, Y.-H.; Ye, L.; Yang, G.-Y. *Inorg. Chem. Commun.* **2004**, *7*, 58−61. (d) Zheng, S.-T.; Zhang, J.; Li, B.; Yang, G.-Y. *Dalton Trans.* **2008**, 5584−5587. (e) Zheng, S.-T.; Zhang, J.; Xu, J.-Q.; Yang, G.-Y. *J. Solid State Chem.* **2005**, *178*, 3740−3746. (f) Qi, Y.; Li, Y.; Wang, E.; Jin, H.; Zhang, Z.; Wang, X.; Chang, S. *Inorg. Chim. Acta* **2007**, *360*, 1841−1853.

(4) (a) Antonova, E.; Näther, C.; Kögerler, P.; Bensch, W. *Angew. Chem., Int. Ed.* **2011**, *50*, 764−767. (b) Zhang, L.; Zhao, X.; Xu, J.; Wang, T. *J. Chem. Soc., Dalton Trans.* **2002**, 3275−3276. (c) Wutkowski, A.; Näther, C.; Kögerler, P.; Bensch, W. *Inorg. Chem.* **2008**, *47*, 1916−1918. (d) Wutkowski, A.; Näther, C.; Kögerler, P.; Bensch, W. *Inorg. Chem.* **2013**, *52*, 3280−3284. (e) Hu, X.; Xu, J.; Cui, X.; Song, J.; Wang, T. *Inorg. Chem. Commun.* **2004**, *7*, 264−267. (f) Kiebach, R.; Näther, C.; Bensch, W. *Solid State Sci.* **2006**, *8*, 964−970. (g) Antonova, E.; Wutkowski, A.; Näther, C.; Bensch, W. *Solid State Sci.* **2011**, *13*, 2154−2159.

(5) (a) Whitfield, T.; Wang, X.; Jacobson, A. J. *Inorg. Chem.* **2003**, *42*, 3728−3733. (b) Wang, J.; Näther, C.; Kögerler, P.; Bensch, W. *Inorg. Chim. Acta* **2010**, *10*, 4399−4404. (c) Pitzschke, D.; Wang, J.; Hoffmann, R.-D.; Pöttgen, R.; Bensch, W. *Angew. Chem., Int. Ed.* **2006**, *45*, 1305−1308. (d) Chen, Y.-M.; Wang, E.-B.; Lin, B.-Z.; Wang, S.-T. *Dalton Trans.* **2003**, 519−520. (e) Gao, Y.; Xu, Y.; Cao, Y.; Hu, C. *Dalton Trans.* **2012**, *41*, 567−571. (f) Wang, X.; Liu, L.; Zhang, G.; Jacobson, A. J. *Chem. Commun.* **2001**, 2472−2473.

(6) (a) Tripathi, A.; Hughbanks, T.; Clearfield, A. *J. Am. Chem. Soc.* **2003**, *125*, 10528−10529. (b) Gao, Y.; Xu, Y.; Huang, K.; Han, Z.; Hu, C. *Dalton Trans.* **2012**, *41*, 6122−6129. (c) Zhou, J.; Zhang, J.; Fang, W.-H.; Yang, G.-Y. *Chem.—Eur. J.* **2010**, *16*, 13253−13261.

(7) (a) Zheng, S.-T.; Zhang, J.; Yang, G.-Y. *Inorg. Chem.* **2005**, *44*, 2426−2430. (b) Zheng, S.-T.; Zhang, J.; Yang, G.-Y. *Eur. J. Inorg. Chem.* **2004**, 2004−2007. (c) Zheng, S.-T.; Chen, Y.-M.; Zhang, J.; Xu, J.-Q.; Yang, G.-Y. *Eur. J. Inorg. Chem.* **2006**, 397−406. (d) Cui, X.-B.; Xu, J.-Q.; Meng, H.; Zheng, S.-T.; Yang, G.-Y. *Inorg. Chem.* **2004**, *43*, 8005−8009. (e) Zheng, S.-T.; Wang, M.-H.; Yang, G.-Y. *Inorg. Chem.* **2007**, *46*, 9503−9508.

(8) (a) Qi, Y.; Li, Y.; Qin, C.; Wang, E.; Jin, H.; Xiao, D.; Wang, X.; Chang, S. *Inorg. Chem.* **2007**, *46*, 3217−3230. (b) Qi, Y.; Li, Y.; Wang, E.; Zhang, Z.; Chang, S. *Dalton Trans.* **2008**, 2335−2345.

(9) (a) Soghomonian, V.; Chen, Q.; Haushalter, R. C.; Zubieta, J. *Angew. Chem. Int. Ed.* **1993**, *32*, 610−612. (b) Haushalter, R. C.; Wang, J. Z.; Thompson, M. E.; Zubieta, J. *Inorg. Chem.* **1993**, *32*, 370−3704. (c) Haushalter, R. C.; Wang, Z.; ThompSon, M. E.; Zubieta, J.; O'Connor, C. J. *Inorg. Chem.* **1993**, *32*, 3966−3969. (d) Tidmarsh, I. S.; Laye, R. H.; Brearley, P. R.; Shanmugam, M.; Sanudo, E. C.; Sorace, L.; Caneschi, A.; McInnes, E. J. L. *Chem. Commun.* **2006**, 2560−2562.

(10) Aronica, C.; Zueva, G.; Chastanet; Zueva, E.; Borshch, S. A.; Clemente-Juan, J. M.; Luneau, D. *J. Am. Chem. Soc.* **2008**, *130*, 2365−2371.

(11) (a) Darkwa, J.; Lockemeyer, J. R.; Boyd, P. D. W.; Rauchfuss, T. B.; Rheingold, A. L. *J. Am. Chem. Soc.* **1988**, *110*, 141−149. (b) Cotton, F. A.; Duraj, S. A.; Roth, W. J. *Inorg. Chem.* **1984**, *23*, 4042−4045. (c) Duraj, S. A.; Andras, M. T.; Rihter, B. *Polyhedron* **1989**, *8*, 2763−2767. (d) Pasynskii, A. A.; Eremenko, I. L.; Katugin, A. S.; Gasanov, G. S.; Turchanova, E. A.; Ellert, O. G.; Struchkov, Y. T.; Shklover, V. E.; Berberova, N. T.; Sogomonova, A. G.; Okhlobystin, O. Y. *J. Organomet. Chem.* **1988**, *344*, 195−213.

(12) (a) Liu, Y.; Chen, Z.; Shi, S.; Luo, H.; Zhong, D.; Zou, H.; Liang, H. *Inorg. Chem. Commun.* **2007**, *10*, 1269−1272. (b) Tidmarsh, I. S.; Scales, E.; Brearley, P. R.; Wolowska, J.; Sorace, L.; Caneschi, A.; Laye, R. H.; McInnes, E. J. L. *Inorg. Chem.* **2007**, *46*, 9743−9753. (c) Jiang, F.; Anderson, O. P.; Miller, S. M.; Chen, J.; Mahroof-Tahir, M.; Crans, D. C. *Inorg. Chem.* **1998**, *37*, 5439−5451. (d) Sanudo, E. C.; Smith, A. A.; Mason, P. V.; Helliwell, M.; Aromí, G.; Winpenny, R. E. P. *Dalton Trans.* **2006**, 1981−1987. (e) Zhu, H.; Liu, Q.; Chen, C.; Wu, D. *Inorg. Chim. Acta* **2000**, *306*, 131−136. (f) Zheng, L.; Wang, X.; Wang, Y.; Jacobson, A. J. *J. Mater. Chem.* **2001**, *11*, 1100−1105.

(13) (a) Brown, I. D.; Wu, K. K. *Acta Crystallogr.* **1976**, *B32*, 1957−1959. (b) Brown, I. D.; Altermatt, D. *Acta Crystallogr.* **1985**, *B41*, 244−247. (c) Brese, N. E.; O'Keeffe, M. *Acta Crystallogr.* **1991**, *B47*, 192−197.

(14) Silversmit, G.; Depla, D.; Poelman, H.; Marin, G. B.; De Gryse, R. *J. Electron Spectrosc. Relat. Phenom.* **2004**, *135*, 167−175.

(15) Centrone, A.; Yang, Y.; Speakman, S.; Bromberg, L.; Rutledge, G. C.; Hatton, T. A. *J. Am. Chem. Soc.* **2010**, *132*, 15687−15691.

(16) (a) Huang, C.-H.; Huang, L.-H.; Lii, K.-H. *Inorg. Chem.* **2001**, *40*, 2625−2627. (b) Xu, L.; Lu, M.; Xu, B.; Wei, Y.; Peng, Z.; Powell, D. R. *Angew. Chem., Int. Ed.* **2002**, *41*, 4129−4132.

(17) (a) Khan, M. I.; Yohannes, E.; Powel, D. *Chem. Commun.* **1999**, 23−24. (b) Do, J.; Bontchev, R. P.; Jacobson, A. J. *Inorg. Chem.* **2000**, *39*, 4305−4310.

(18) (a) Sha, J.; Peng, J.; Liu, H.; Chen, J.; Tian, A.; Zhang, P. *Inorg. Chem.* **2007**, *46*, 11183−11189. (b) Pichon, C.; Dolbecq, A.; Mialane, P.; Marrot, J.; Rivière, E.; Goral, M.; Zynek, M.; McCormac, T.; Borshch, S. A.; Zueva, E.; Sécheresse, F. *Chem.—Eur. J.* **2008**, *14*, 3189−3199.

(19) Müller, A.; Das, S. K.; Bogge, H.; Beugholt, C.; Schmidtmann, M. *Chem. Commun.* **1999**, 1035−1036.

(20) (a) Khan, M. I.; Meyer, L. M.; Haushalter, R. C.; Schweitzer, A. L.; Zubieta, J.; Dye, J. L. *Chem. Mater.* **1996**, *8*, 43−53. (b) Behrens, E. A.; Poojary, D. M.; Clearfield, A. *Chem. Mater.* **1996**, *8*, 1236−1244.
(21) Plévert, J.; Sanchez-Smith, R.; Gentz, T. M.; Li, H.; Groy, T. L.; Yaghi, O. M.; O'Keeffe, M. *Inorg. Chem.* **2003**, *42*, 5954−5959.
(22) Liu, Z.; Weng, L.; Chen, Z.; Zhao, D. *Inorg. Chem.* **2003**, *42*, 5960−5965.
(23) Francis, R. J.; Jacobson, A. J. *Chem. Mater.* **2001**, *13*, 4676−4680.
(24) Lin, Z.-E.; Zhang, J.; Zheng, S.-T.; Yang, G.-Y. *Micropor. Mesopor. Mat.* **2004**, *74*, 205−211.